

12-2018

Fiber element-based nonlinear analysis of concrete bridge piers with consideration of permanent displacement

Mokhtar Ansari

Bozorgmehr University of Qaenat

Farhad Daneshjoo

Tarbiat Modares University

Amir Safiey

Clemson University, asafiey@g.clemson.edu

Naser Safaeian Hamzehkolaei

Bozorgmehr University of Qaenat

Maryam Sorkhou

Gilan University

Follow this and additional works at: https://tigerprints.clemson.edu/elec_comp_pubs



Part of the [Civil and Environmental Engineering Commons](#)

Recommended Citation

Ansari, Mokhtar; Daneshjoo, Farhad; Safiey, Amir; Hamzehkolaei, Naser Safaeian; and Sorkhou, Maryam, "Fiber element-based nonlinear analysis of concrete bridge piers with consideration of permanent displacement" (2018). *Publications*. 14.

https://tigerprints.clemson.edu/elec_comp_pubs/14

This Article is brought to you for free and open access by the Holcombe Department of Electrical & Computer Engineering at TigerPrints. It has been accepted for inclusion in Publications by an authorized administrator of TigerPrints. For more information, please contact kokeefe@clemson.edu.

Fiber element-based nonlinear analysis of concrete bridge piers with consideration of permanent displacement

Mokhtar Ansari*¹, Farhad Daneshjoo^{2a}, Amir Safiey^{3b}, Naser Safaeian Hamzehkolaei^{1c}
and Maryam Sorkhou^{4d}

¹Department of Civil Engineering, Bozorgmehr University of Qaenat, Qaen, Iran

²Department of Civil Engineering, Tarbiat Modares University, Tehran, Iran

³Glenn Department of Civil Engineering, Clemson University, Clemson, USA

⁴Department of Civil Engineering, Gilan University, Rasht, Iran

(Received October 25, 2018, Revised December 27, 2018, Accepted December 30, 2018)

Abstract. Utilization of fiber beam-column element has gained considerable attention in recent years due mainly to its ability to model distributed plasticity over the length of the element through a number of integration points. However, the relatively high sensitivity of the method to modeling parameters as well as material behavior models can pose a significant challenge. Residual drift is one of the seismic demands which is highly sensitive to modeling parameters and material behavior models. Permanent deformations play a prominent role in the post-earthquake evaluation of serviceability of bridges affected by a near-fault ground shaking. In this research, the influence of distributed plasticity modeling parameters using both force-based and displacement-based fiber elements in the prediction of internal forces obtained from the nonlinear static analysis is studied. Having chosen suitable type and size of elements and number of integration points, the authors take the next step by investigating the influence of material behavioral model employed for the prediction of permanent deformations in the nonlinear dynamic analysis. The result shows that the choice of element type and size, number of integration points, modification of cyclic concrete behavior model and reloading strain of concrete significantly influence the fidelity of fiber element method for the prediction of permanent deformations.

Keywords: distributed plasticity; permanent displacements; displacement-based and force-based fiber element; integration point; material behavior model; reloading strain of concrete

1. Introduction

The need for tracing the nonlinear behavior of reinforced concrete structures all through to the onset of collapse led to the emergence of different analytical and numerical techniques (Li *et al.* 2012). There are a variety of modeling techniques to predict the nonlinear behaviour of reinforced concrete structures. Each method entails unique capabilities, theory, assumptions, reliability and computational time expense (Zendaoui 2016). Some of these methods are not appropriate for practical purposes. Performance-based earthquake engineering of reinforced concrete bridges requires prediction of nonlinear responses due to earthquake excitations (Huang and Kwon 2015 and

Ramin and Fereidoonfar 2015). It is very common to idealize bridge piers as a beam-column element to predict their nonlinear responses. There are several studies conducted on different nonlinear modeling of reinforced concrete piers. Hashemi and Vaghefi studied nonlinear behavior of reinforced concrete frames taking the slip between reinforcement and concrete at joints as well as over the length of the column into account using fiber elements. This study reveals a good agreement between the predictions made using the fiber element and the experimental results (Hashemi and Vaghefi 2015). Du *et al.* divided a beam-column to number of elements, sections and fibers by using three types of elements consisting of displacement, force and plastic hinge elements in order to improve computational efficiency and accuracy (Du *et al.* 2012). Beery and Eberhand presented different strategies to model reinforced concrete piers using fiber elements under earthquake excitations enabling predicting the maximum and permanent deformations together with damage propagations (Beery and Eberhand 2008). Alemdar *et al.* presented A high-resolution model of a bridge column using the computer program ABAQUS, and the accuracy of the model was evaluated for the displacement field and the rotations of a bridge system subjected to shake-table loading. The effect of simulation parameters (reinforcing bar slip within the joint and stiffness degradation of the concrete) was studied to determine the goodness-of-fit of

*Corresponding author, Assistant Professor

E-mail: ansari@buqaen.ac.ir

^aProfessor

E-mail: danesh_fa@modares.ac.ir

^bResearch Assistant

E-mail: asafiey@g.clemson.edu

^cAssistant Professor

E-mail: nsafaeian@buqaen.ac.ir

^dResearch Assistant

E-mail: SorkhouMaryam@gmail.com

the displacement and rotation fields recorded during the dynamic response (Alemdar *et al.* 2013). Phan *et al.* tested a number of reinforced concrete bridge piers under near- and far-field ground motions to investigate and compare their permanent displacements and seismic performance. Eventually, they proposed a simple hysteresis relationship for the prediction of residual drifts (Phan *et al.* 2007). Shu *et al.* presented an innovative method to realistically predict the residual drifts of bilinear bridge deck-column systems directly from their inelastic mechanical properties and ground motion characteristics. The proposed estimation originated from the rigorous dimensional analysis of nonlinear time-history responses of various bilinear bridge deck-column systems under near-fault ground motions (Shu *et al.* 2018). Lee and Billington could eliminate pinching effect from the cyclic behavior of reinforced concrete in the fiber modeling causing errors in the estimation of the residual displacements of bridge piers. They proposed a modified constitutive model for concrete with a reasonable prediction of residual displacements of reinforced concrete piers compared with the shake table test results. However, the proposed model did not perform very well in the prediction of the permanent displacements of prestressed concrete piers (Lee and Billington 2010). Choi *et al.* suggested a new design earthquake spectrum as an alternative for the Caltrans (California Department of Transportation) design earthquake spectrum for near-fault regions. After that, the adequacy of these methods is examined for bridge reinforced concrete piers using shake table tests under near-fault excitations. Finally, they predicted the permanent displacements of piers using a simple hysteresis model (Choi *et al.* 2010). Wang *et al.* and Fahemi *et al.* compared the permanent deformations of cast-in-place and precast ordinary reinforced concrete and prestressed concrete bridge piers exposed to cyclic loading. A model is proposed in order to predict permanent deformations of precast prestressed bridge piers, (Fahmy *et al.* 2010, Wang *et al.* 2011). In these courses of study, various numerical models using fiber elements for predicting maximum and permanent displacements are proposed. A comparison between these models predictions and test results reveals that they perform well for the prediction of maximum displacements but not for permanent displacements and internal member forces.

The distributed plasticity models permit the yielding at any point over the element length. This feature is very important to capture nonlinear behavior of beam-column element subjected to a lateral distributed loading. Constant axial strain and linear curvature are assumed for displacement-based element throughout the member. Pushover analysis requires a finer mesh sizing in order for more efficient simulation of the curvature especially at the ends of the element which are prone to plastic hinge formation. Therefore, it is needed to increase the number of elements to augment accuracy. These elements tend to converge to the exact response more slowly. Also, element sizes need to be refined to enhance the efficiency of the prediction of responses. Noteworthy, element size refinement of displacement-based elements expedite more the convergence of the local responses (e.g., curvature and

axial strain) than global responses (e.g., rotation). As force-based elements regards, both increases in the number of elements and number of integration points lead to increase the accuracy. However, the increase in the number of integration points is usually more preferable from numerical points of view. Both local and global responses tend to converge more rapidly with the increase of number integration points of the force-based elements (Terzic 2011 and Li *et al.* 2012). In essence, both element types can lead to similar results if a proper number of elements and integration points are included. Although most software packages incorporate with displacement-based elements mainly due to the relative ease of implementation, the obtained results are not as precise as those of the force-based method.

Permanent displacement of a bridge pier affected by a strong ground motion is one of the main post-earthquake functionality decision variables (Ansari *et al.* 2017, Bas *et al.* 2016). Near-field earthquakes with directivity effect have more permanent displacement that cause disturbance in serviceability variables (Ansari *et al.* 2018, Huff 2016). In this study, the accuracy of distributed plasticity models in prediction of internal forces of members of bridge piers through nonlinear static analysis is investigated. Having chosen a proper modeling method, the authors take the next step by studying the influence of concrete constitutive law on the prediction of permanent deformations through nonlinear analysis. The previous studies have investigated the influence of the type of the element (force-based or displacement-based) and size of the element on the global responses including the capacity curve obtained from the inelastic static analyses. This paper for the first time investigates the influence of the type and size of the element on the local response of beam-column, e.g., the axial strain, the curvature, as well as stress and strain developed in the fibers within the cross-section of the member. This research took a step further by studying the influence of the element mesh refinement on the local responses in four different levels of displacements defined as a fraction of target displacement of the control point, while the previous studies merely focus on the global responses at the target displacement. Having concluded the proper element size in order for simulation of a bridge pier, this study explores the influence of different material constitutive law on the prediction of the residual displacements which further highlights the significance of reloading strain.

2. Review of force-based and displacement-based fiber element modeling

Lumped plasticity models, also known as phenomenological models, simulate the nonlinear behavior of beam-column elements using zero-length nonlinear springs incorporating with hysteresis force-displacement at two ends of the member. Fiber element can account for the distributed plasticity resulting in a more accurate description of the nonlinear behavior of reinforced concrete beams (Petrone *et al.* 2016, Kampitsis *et al.* 2015, Bahadori *et al.* 2016). On the contrary to phenomenological

modeling, the fiber modeling can have the material nonlinear at any section throughout the member. The behavior of the member is obtainable by weighted integration of the response over the cross-section. In reality, numerical integration is undertaken by which only the response in a select number of points within the section is considered (Karaton 2014, Sadeghi *et al.* 2017). Displacements and forces are the primary unknowns of the model, which can be obtained using proper interpolation functions for element displacements and forces in the global coordinate system (Calabrese *et al.* 2010, Roh *et al.* 2012, Alemdar and White 2005).

In displacement-based finite element method, member deformations are directly predicted from the nodal displacements using deformation interpolation functions. Subsequently, the forces developed in the member can be achieved through the force-displacement relationship of the section. Internal forces of the member can be predicted by weighted integration over the element length, which completes the process of determination of the element state. However, in the force-based finite element formulation, the first step is the determination of element forces using force interpolation functions. Thereafter, the member cross section displacements can be obtained using the obtained forces. Finally, element deformations can be predicted using weighted integration (Huang and Chen 2003, Guyen and Kim 2014).

The first version of distributed plasticity models utilized displacement-based formulation. They use a Hermitian cubic polynomial function denoted as $\varphi(x)$ to predict lateral displacements, and linear function denoted as $\psi(x)$ to predict axial displacements. Fig. 1 presents a displacement-based element with the bending and axial degrees of freedom. These elements are assumed to behave linear elastic for torsional degrees of freedom under both circumstances. In addition, there is no interaction between the axial and bending degrees of freedom. \bar{q} represents the nodal displacement vector of an element in the local coordinates. The x represents the axial vector of the member axis. Transverse and longitudinal displacements, $\theta(x)$ are estimated by $u(x)$ and $v(x)$

$$\bar{q} = \{u_i, v_i, \theta_i, u_j, v_j, \theta_j\} \quad (1)$$

$$\bar{d}(x) = \begin{Bmatrix} u(x) \\ v(x) \end{Bmatrix} = a_d(x) \cdot \bar{q} \quad (2)$$

In the above relationship, $a_d(x)$, is a matrix containing the third degree interpolation function coefficients for transverse displacements and first degree interpolation function for axial displacements.

$$a_d(x) = \begin{bmatrix} \Psi_1(x) & 0 & 0 & \Psi_2(x) & 0 & 0 \\ 0 & \varphi_1(x) & \varphi_2(x) & 0 & \varphi_3(x) & \varphi_4(x) \end{bmatrix} \quad (3)$$

$$\bar{d}(x) = \begin{Bmatrix} u(x) \\ v(x) \end{Bmatrix} = a_d(x) \cdot \bar{q} \quad (4)$$

$$\varphi_1(x) = 2 \frac{x^3}{L^3} - 3 \frac{x^2}{L^2} + 1 \quad (5)$$

and

$$\varphi_2(x) = \frac{x^3}{L^2} - 2 \frac{x^2}{L} + x$$

$$\varphi_3(x) = \frac{x^3}{L^2} - \frac{x^2}{L} \quad (6)$$

and

$$\varphi_4(x) = -2 \frac{x^3}{L^3} + 3 \frac{x^2}{L^2}$$

Section displacements or generalized displacements $\bar{d}(x)$ including axial strain $\epsilon(x)$ and curvature in respect to z-axis, $\chi_z(x)$ can be related to nodal displacements using the following relationships. In these relationships, $\bar{a}(x)$ can be obtained by displacement interpolation functions.

$$\bar{d}(x) = \begin{Bmatrix} \epsilon(x) \\ \chi_z(x) \end{Bmatrix} = \begin{Bmatrix} u'(x) \\ v''(x) \end{Bmatrix} = \bar{a}(x) \cdot \bar{q} \quad (7)$$

$$\bar{a}(x) = \begin{bmatrix} \Psi_1'(x) & 0 & 0 & \Psi_2'(x) & 0 & 0 \\ 0 & \varphi_1''(x) & \varphi_2''(x) & 0 & \varphi_3''(x) & \varphi_4''(x) \end{bmatrix} \quad (8)$$

In this formulation, the virtual displacement method is used to calculate the stiffness matrix, \bar{K} , by integration of the cross-sectional stiffness, $k(x)$. Cross-sectional forces, $D(x)$, are predicted by the multiplication of cross-sectional stiffness, $k(x)$, to the corresponding cross-sectional deformations, $\bar{d}(x)$. The cross-sectional generalized forces are axial forces, $N(x)$, and bending moments, $M(x)$, at x . The resisting forces of the section, $Q_R(x)$, is calculated by integration from the cross-sectional forces, $D_R(x)$, using the principle of virtual work.

$$\bar{K} = \int_0^{L-T} \bar{a}^T(x) \cdot k(x) \cdot \bar{a}(x) \cdot dx \quad (9)$$

$$D(x) = k(x) \cdot \bar{d}(x) \quad (10)$$

$$D(x) = \begin{Bmatrix} N(x) \\ M_z(x) \end{Bmatrix} \quad (11)$$

$$\bar{Q}_R = \int_0^{L-T} \bar{a}^T(x) \cdot D_R(x) \cdot dx \quad (12)$$

The main shortcoming of the displacement-based elements is their inability to describe the nonlinear behavior of the element at the neighborhood of its ultimate strength

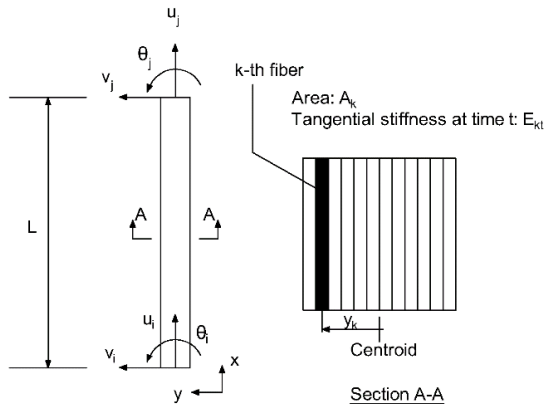


Fig. 1 Geometry of displacement-based fiber element

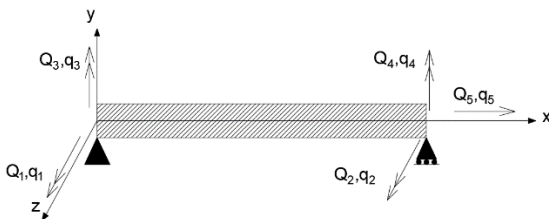


Fig. 2 Geometry of force-based beam column fiber element without rigid motion modes (adopted from Taucer et al. 1991)

as well as beyond the strain softening. This issue is more critical for near-fault ground motions which can trigger greater residual displacements. The curvature of a member with plastic hinges developed at both ends cannot be approximated by displacement-based elements by third-degree Hermitian functions effectively. One of the main limitations of the classic version of the displacement-based method is the utilization of the third-degree interpolation functions. This assumption can result in the linear distribution of the curvature over the length of the element. This assumption leads to reasonable results within linear or near linear responses. However, the linear distribution of the curvature becomes highly inelastic when a reinforced concrete member is extensively yielded at both ends. Therefore, a great deal of finesse is necessary for discretization of a structure to predict nonlinear responses when using the stiffness method.

The force-based method utilizes force interpolation functions within the element. Fig. 2 shows generalized displacements including the end rotations and axial displacements without rigid movement modes of the element. The vector of element force without rigid modes under uniaxial bending is (Alemdar et al. 2005, Huang and Chen 2003)

$$Q = \{Q_1, Q_2, Q_3\} \tag{13}$$

It is common to assume the flexural forces are distributed linearly, and the axial forces are constant over the length of the element. In vector space

$$D(x) = b(x).Q \tag{14}$$

where $b(x)$ matrix contains force interpolation functions.

$$b(x) = \begin{bmatrix} 0 & 0 & 1 \\ \frac{x}{L} - 1 & \frac{x}{L} & 0 \end{bmatrix} \tag{15}$$

The flexibility matrix of the element is obtainable using the principle of virtual work as follows

$$F = \int_0^L b^T(x).f(x).b(x).dx \tag{16}$$

where $f(x)$ is the flexibility matrix of the section as follows

$$d(x) = f(x).D(x) \tag{17}$$

One of the advantages of the flexibility method is the fact that force interpolation functions satisfy the equilibrium regardless of the element state. The condition is no force is being applied over the length of the element. In other words, the assumed distribution for internal element forces are precise and realistic and has no relationship with the nonlinearization of the material over the depth of the section. Even onset of softening beyond the ultimate strength does not influence the distribution of forces.

3. Modeling of the experimental bridge pier

An experimental bridge pier as shown in Fig. 3 tested with 4/5 scale specimen is undertaken. This experimental bridge pier is modeled using fiber elements in order for comparison of different local responses rendered by nonlinear static analyses, the prediction of the permanent deformations of the bridge pier obtained from time history analyses and an investigation into the reliability of the results. The bridge pier cross-section is discretized into 252 fibers (200 fibers for core concrete, 40 fibers for concrete cover and 12 fibers for steel reinforcements). Fig. 4 presents the fiber discretization of the specimen cross-section schematically.

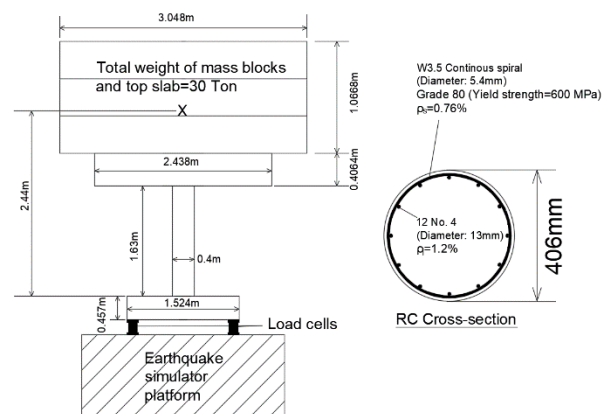


Fig. 3 Schematic geometry of scaled-down specimen (adopted from Jeong et al. 2008)

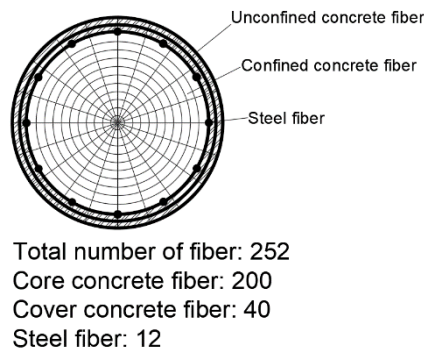


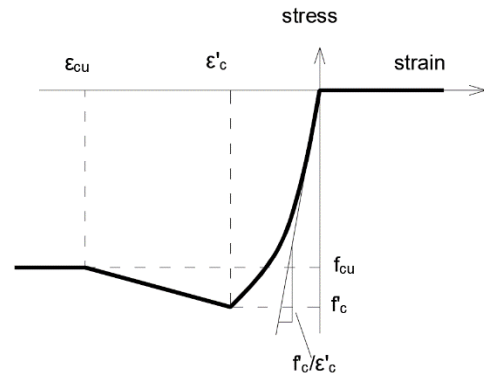
Fig. 4 Idealization of the bridge pier using fiber elements

4. Influence of steel and concrete characteristic relationships

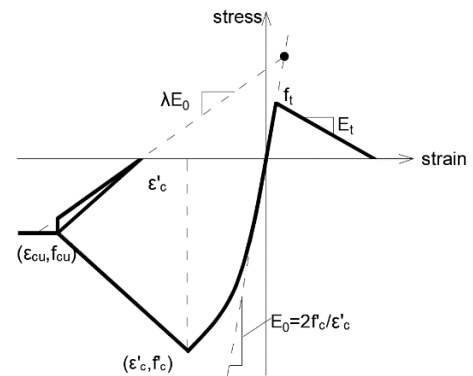
Three different concrete material model as shown in Fig. 5 is employed for the core and cover concrete.

Concrete model-1 is the uniaxial Kent-Scott-Park concrete model incorporating with Karsan-Jirsa in order for reduction of the unloading and reloading stiffness (Karsan and Jirsa 1969). The tensile strength of the concrete is ignored in this model. Concrete model-2 is the modified version of the concrete model-1 by taking the tensile strength into account in conjunction with the linear softening in the tensile region. Concrete model-3 which is the focus of this study is the same as concrete model-1 with a dissimilar unloading and reloading strain for hysteresis model of the concrete. This model is a modified version of Stanton and McNiven model. The reloading and unloading strains are not the same on two grounds. First, the crushed material (aggregates and cement paste) due to cracking can fill the developed openings in the concrete in the cycles of loadings and reloading. Second, the crack closure within cycles of loadings and reloading happens in a way that the cracked material with closed cracks does not behave the same as the intact concrete. Therefore, the stress transfer mechanisms are different from similar concrete models by differentiating the reloading strain from unloading strain. Concrete model-3 is modified to account for these effects by a reloading strain (ϵ_r) takes place earlier than the unloading strain (ϵ_{cul}). In this model, the reloading strain is constant calibrated by test results.

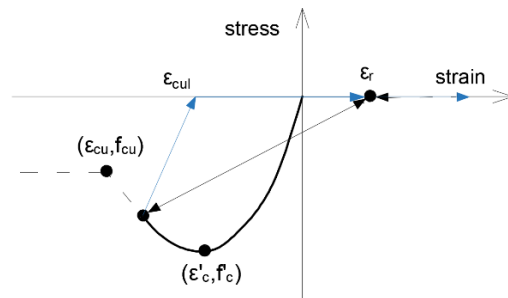
Whereas the strength of the core concrete of the bridge is higher than that of the cover concrete, Mander relationship is employed to estimate the maximum concrete compressive stress and strain of the confined concrete (concrete core) to account for the influence of spiral stirrups confinement (Mander and Cheng 1997). Longitudinal reinforcements of the bridge pier are modeled using two models: Reinforcing steel and Steel02. Model Steel02 is the same as Giuffre-Menegotto-Pinto combined model. This model is a bilinear curve in which the stiffness after yielding is considered as a fraction of the initial elastic moduli. This model incorporates with the Bauschinger effect, which plays an essential role in stiffness deterioration of reinforced concrete members under cyclic loadings. This model includes an isotropic stiffening in



(a) Concrete model 1



(b) Concrete model 2



(c) Concrete model 3 (adopted from Kim *et al.* 2010)

Fig. 5 Concrete behavior models: (a) model without considering tension (b) model including tensile strength and linear tensile softening (c) concrete model including aggregates trapped in the aggregate (Stanton and McNiven model)

tension and compression for the hysteresis curve. The steel02 model also incorporates the steel strength deterioration due to buckling and the rupture of the longitudinal reinforcement. Reinforcing steel model can capture the reinforcement buckling considering the slenderness of the reinforcement between two successive ties as shown in Fig. 6.

The size of elements used for the nonlinear modeling of a bridge pier is one of the influential parameters on the prediction of the seismic demands. It is very probable to arrive at unrealistic responses without enough knowledge about the properties and types of elements available for distributed plasticity model approach. In this section, the bridge pier is modeled using two types of force-based and

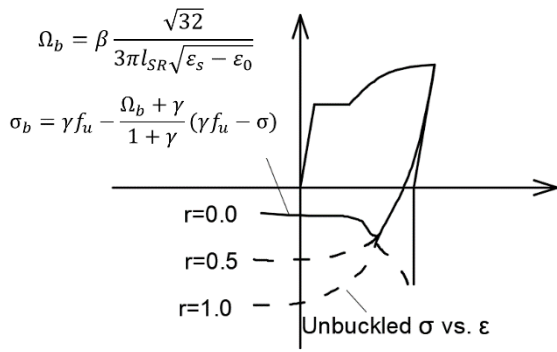


Fig. 6 Reinforcement behavior model including reinforcement buckling (OpenSees 2008)

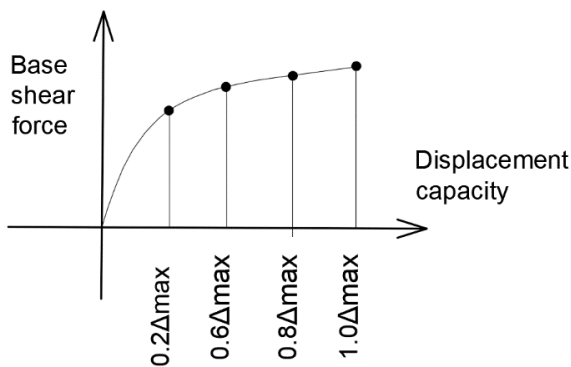


Fig. 7 Nonlinear static analysis and different displacement steps

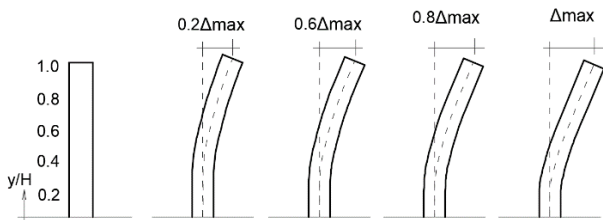


Fig. 8 Displacement steps through nonlinear static analysis

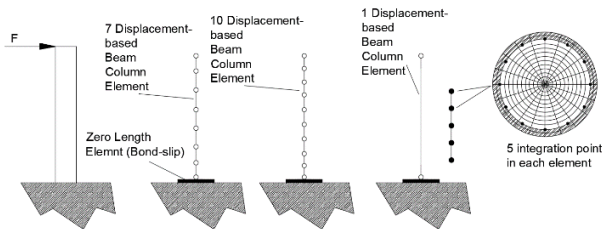


Fig. 9 Modeling of bridge pier using 7 and 10 using displacement-based elements

displacement-based elements. The appropriate element discretization for each type of element is obtained. Firstly, the bridge pier is discretized into 1, 7 and 10 displacement-based elements to compare the accuracy of the predictions. Next, the same comparison is conducted for the force-based elements. This comparison is performed using nonlinear

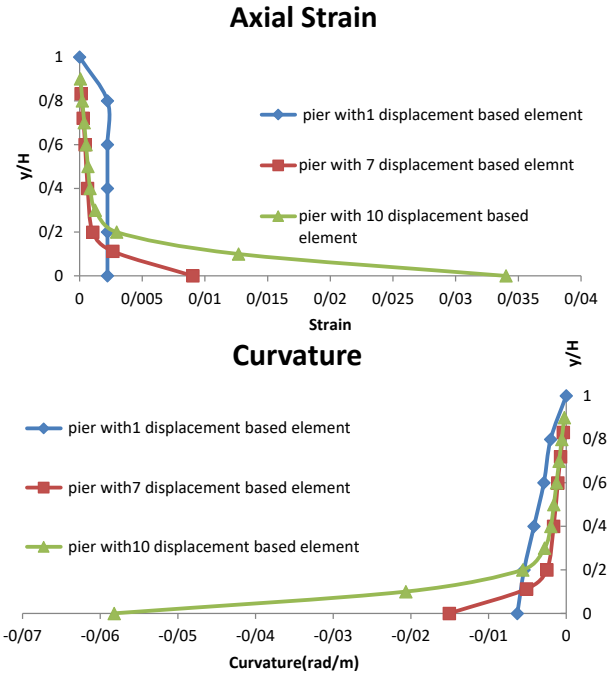


Fig. 10 Comparison between axial strain and curvature using 1, 7, 10 displacement-based elements over the length of the bridge pier at 20.0% of maximum displacement

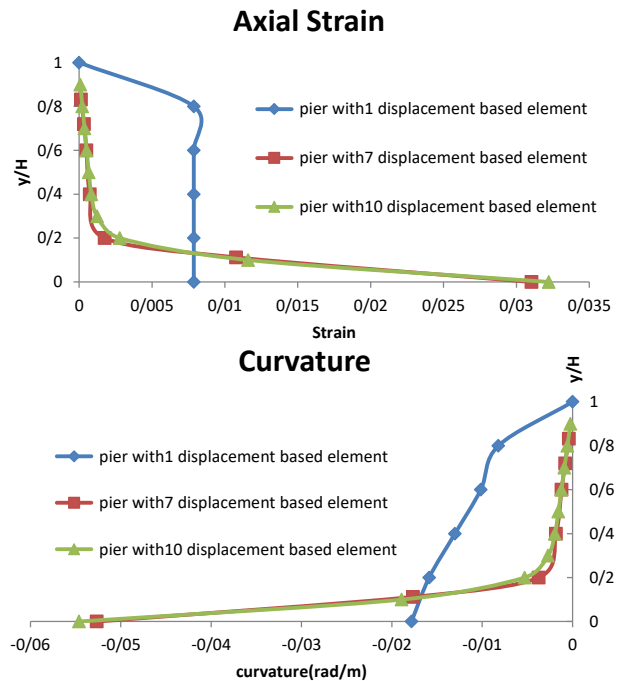


Fig. 11 Comparison between axial strain and curvature using 1, 7, 10 displacement-based elements over the length of the bridge pier at 60.0% of maximum displacement

static analysis. Curvature, axial strain and axial stress and strain at two ends of each element is recorded in order to plot each response over the height of the bridge pier for four levels of displacement (0.2Δmax, 0.6Δmax, 0.8Δmax, and Δmax) as shown in Figs. 7 and 8. Δmax represents the maximum displacement obtained from the nonlinear static analysis.

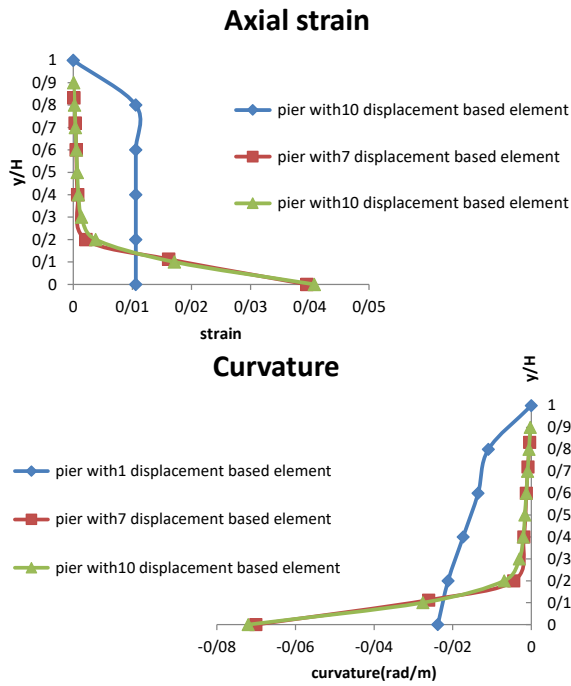


Fig. 12 Comparison between axial strain and curvature using 1, 7, 10 displacement-based elements over the length of the bridge pier at 80.0% of maximum displacement

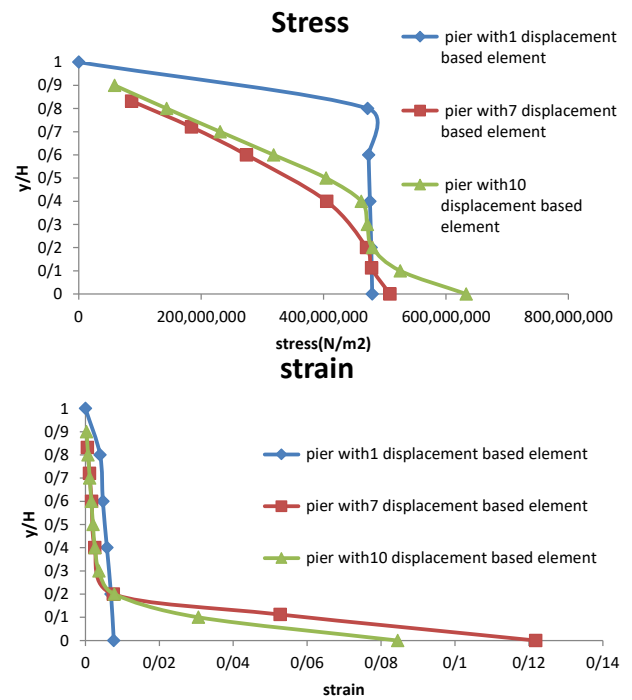


Fig. 14 Comparison between steel strain and stress using 1, 7, 10 displacement-based elements over the length of the bridge pier at 20.0% of maximum displacement

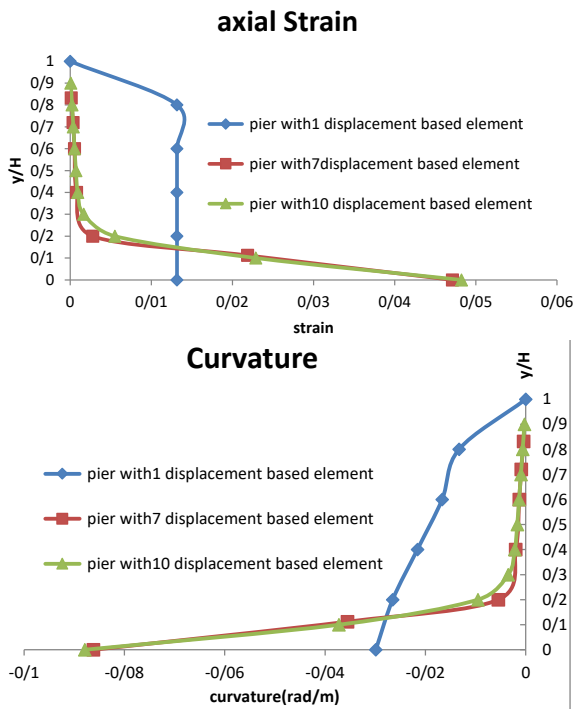


Fig. 13 Comparison between axial strain and curvature using 1, 7, 10 displacement-based elements over the length of the bridge pier at 100.0% of maximum displacement

5. Influence of element size and number of integration points using the distributed plasticity method for nonlinear static analysis

5.1 Investigation into the number of elements in displacement-based approach for bridge pier modeling

The result nonlinear static analyses in different levels are computed and compared in order for studying the influence of element size and the number of integration points on the seismic demands of the bridge piers. The bridge pier is idealized by 1, 7 and 10 displacement-based element as shown in Fig. 9. Each element entails five integration points as shown in Fig. 9 as follows: two points at both ends and three points in the middle.

Variations in axial strain and curvature over the length of the bridge pier are plotted. The vertical axis is the ratio of y/H , and the horizontal axis is either axial strain or curvature in these plots. y is the distance from the origin and H is the total height. Fig. 10 to 13 presents these plots at different stages ($0.2\Delta_{max}$, $0.6\Delta_{max}$, $0.8\Delta_{max}$ and Δ_{max}) of nonlinear static analyses.

A comparison between the variations of axial strains and curvature profiles over the height of the bridge pier reveal the low accuracy of bridge piers modeled only by one element. The rate of curvature and axial strain at the element end (joint with foundation) is considerably lower than the corresponding predictions rendered using 7 and 10 elements. Noteworthy, the increase in the number of displacement-based elements from 7 to 10 does not have considerable influence on the results.

In order to make certain about the low accuracy of the model with a single displacement-based element, plots of strain and steel strain profiles in tensile fiber at $0.2\Delta_{max}$, $0.6\Delta_{max}$, $0.8\Delta_{max}$ and Δ_{max} steps as shown in Fig. 14 to 17 are presented. Similarly, the vertical axis is the ratio of y/H , and the horizontal axis is either axial strain or curvature. y is the distance from the origin and H is the total height.

The result shows that the model with a single

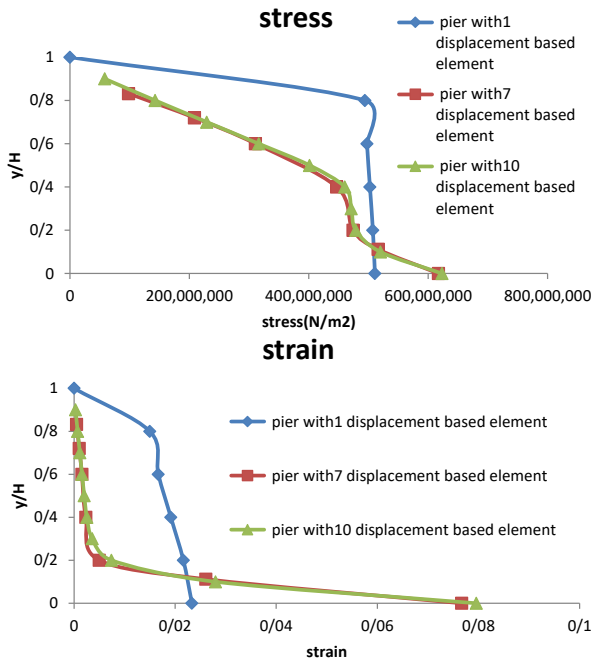


Fig. 15 Comparison between steel strain and stress using 1, 7, 10 displacement-based elements over the length of the bridge pier at 60.0% of maximum displacement

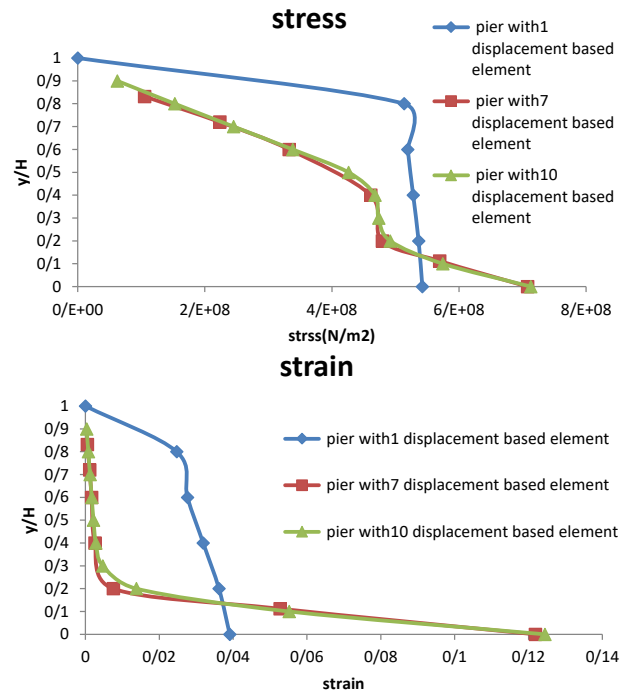


Fig. 17 Comparison between steel strain and stress using 1, 7, 10 displacement-based elements over the length of the bridge pier at 100.0% of maximum displacement

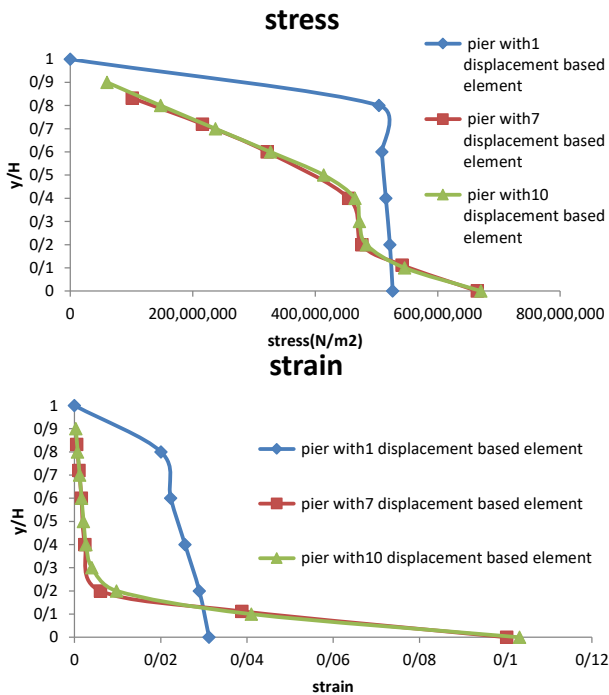


Fig. 16 Comparison between steel strain and stress using 1, 7, 10 displacement-based elements over the length of the bridge pier at 80.0% of maximum displacement

displacement-based element results in low accuracy predictions of strains and stresses, especially at the end of the bridge pier. The increase in the number of elements from 7 to 10 does not change the accuracy for displacement-based elements. Therefore, an increase in the number of displacement-based elements results in a satisfactory efficiency.

5.2 Investigation into the number of elements in force-based approach for bridge pier modeling

In order for investigating the influence of the element size and integration points on the prediction of seismic demands of bridge piers, the result of nonlinear static analyses in different levels is obtained and compared. The bridge pier is discretized into 1, 7 and 10 forced-based elements as shown in Fig. 18. Five integration points are utilized for each element, two at each end and three in the middle, as shown in Fig. 18.

Figs. 19 to 22 presents the variation of the axial strain and curvature over the length of the bridge pier in which the vertical axis is the ratio of y/H , and the horizontal axis is either axial strain or curvature. y is the distance from the origin and H is the total height. These profiles in different levels of nonlinear static analysis ($0.2\Delta_{max}$, $0.6\Delta_{max}$, $0.8\Delta_{max}$, and Δ_{max}) are shown in Figs. 19 to 22.

A comparison between the variation in axial strains and the curvature over the length of the bridge pier shows the profile of variation of these two parameters are close when force-based elements are utilized. In other words, the bridge pier element discretization has a minimal influence on the result for this type of elements.

Similar to the previous section, in order for investigating the influence of the force-based elements on the accuracy of the predicted seismic responses, the stresses and strains of the longitudinal steel reinforcement in the outmost tensile fiber is plotted for $0.2\Delta_{max}$, $0.6\Delta_{max}$, $0.8\Delta_{max}$ and Δ_{max} steps. The horizontal axis of the plots shown in Fig. 23 to Fig. 26 is the steel strains and stresses in the outmost fiber, and the vertical axis of these plots is the y/H ratio.

Examination of strain profile variation plots reveals that

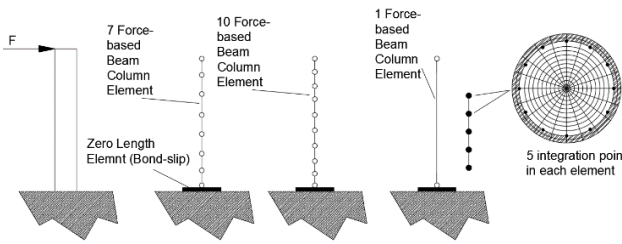


Fig. 18 Modeling of bridge pier with 7 and 10 force-based elements

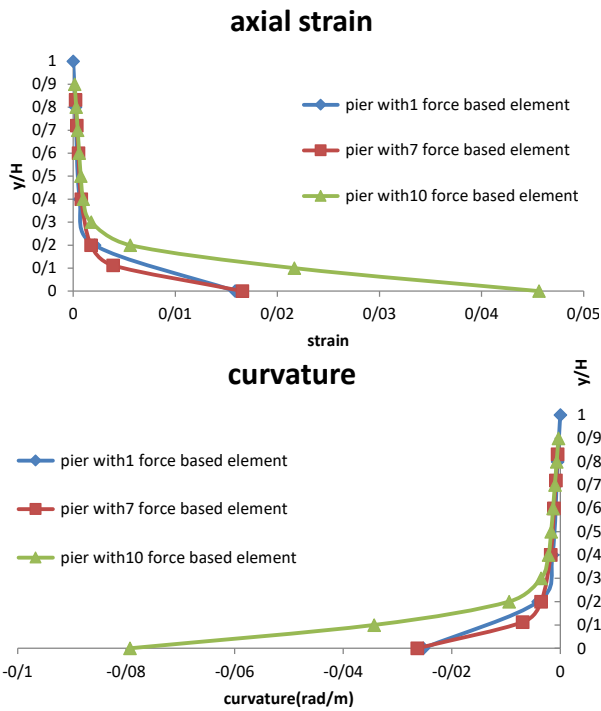


Fig. 19 Comparison between axial strain and curvature using 1, 7, 10 force-based elements over the length of the bridge pier at 20.0% of maximum displacement

the modeling with a single force-based element provides sufficient accuracy compared with discretization with 7 to 10 elements. In other words, modeling using force-based elements exhibits a lower sensitivity to the size of the element used for modeling of the bridge pier.

Higher accuracy can be attained by discretization of the bridge pier into several elements using displacement-based elements which is closer to the results obtained using force-based elements. Fig. 27 is a plot of the variation of axial strains and curvature over the height of the bridge pier using displacement-based and force-based elements. Fig. 28 compares the plots of variations in the strain and stress at the outmost tensile fiber of the steel for both cases of force-based and displacement-based elements. Noteworthy, this comparison is made for a bridge pier model discretized into 10 elements.

The result of the simulation using 10 forced-based and displacement-based elements are very close. Only in the plastic hinge region, the magnitudes of axial strains, curvature, stress, and strain of the steel rendered by force-based elements exceeds those of displacement-based elements.

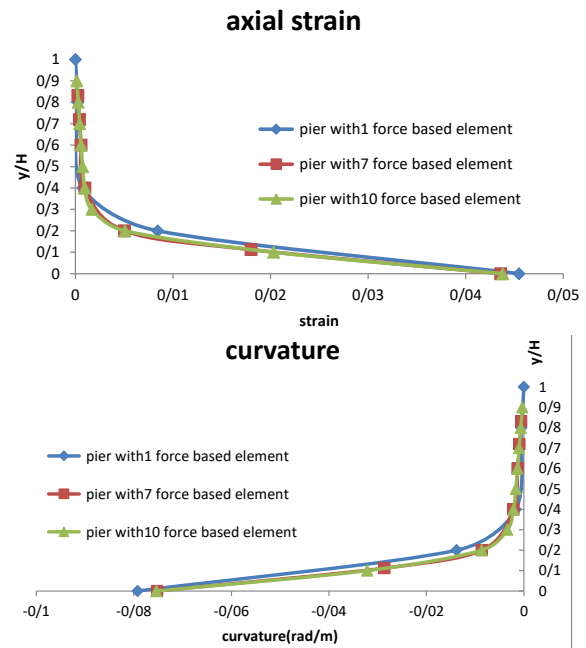


Fig. 20 Comparison between axial strain and curvature using 1, 7, 10 force-based elements over the length of the bridge pier at 60.0% of maximum displacement

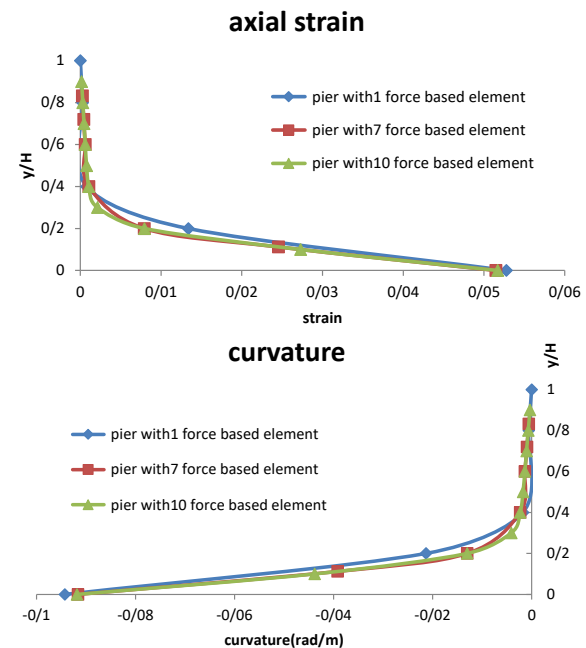


Fig. 21 Comparison between axial strain and curvature using 1, 7, 10 force-based elements over the length of the bridge pier at 80.0% of maximum displacement

The result of nonlinear static analysis of the bridge pier reveals that the displacement-based element needs to be refined adequately to be able to capture the curvatures and the axial strains accurately. However, force-based beam-column elements are more accurate for prediction of strains and curvatures. It is chosen to use 10 distributed plasticity fiber beam column force-based element with 5 integration points. Gauss Lobatto integration method is incorporated in the selected distributed plasticity model to model the

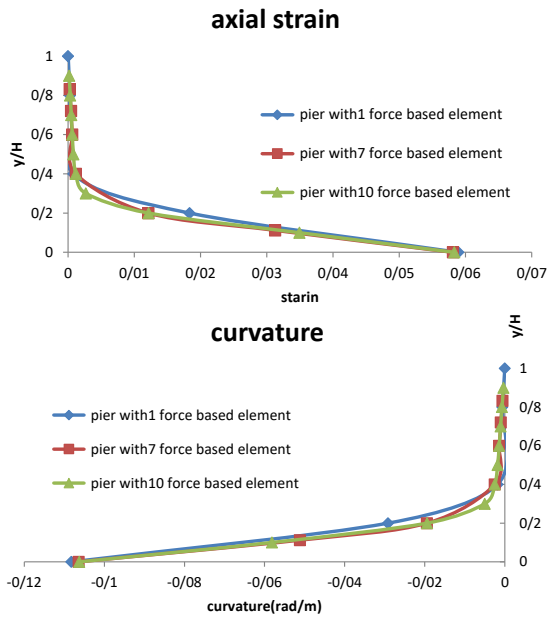


Fig. 22 Comparison between axial strain and curvature using 1, 7, 10 force-based elements over the length of the bridge pier at 100.0% of maximum displacement

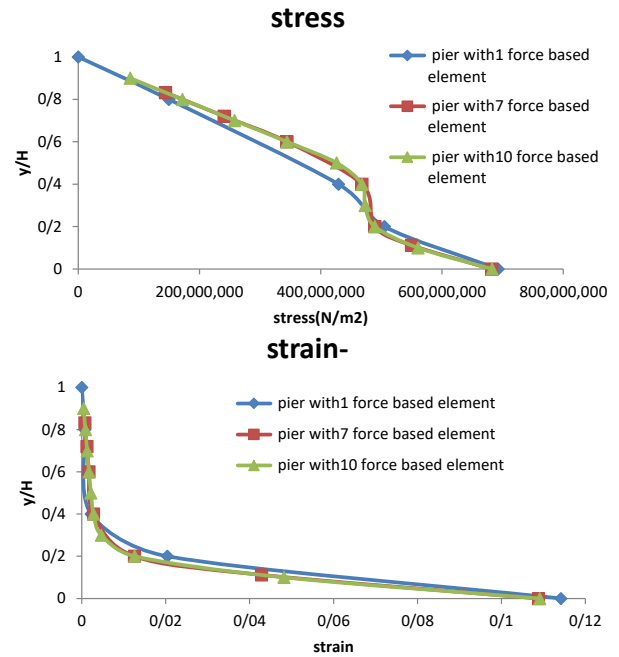


Fig. 24 Comparison between steel strain and stress using 1, 7, 10 force-based elements over the length of the bridge pier at 60.0% of maximum displacement

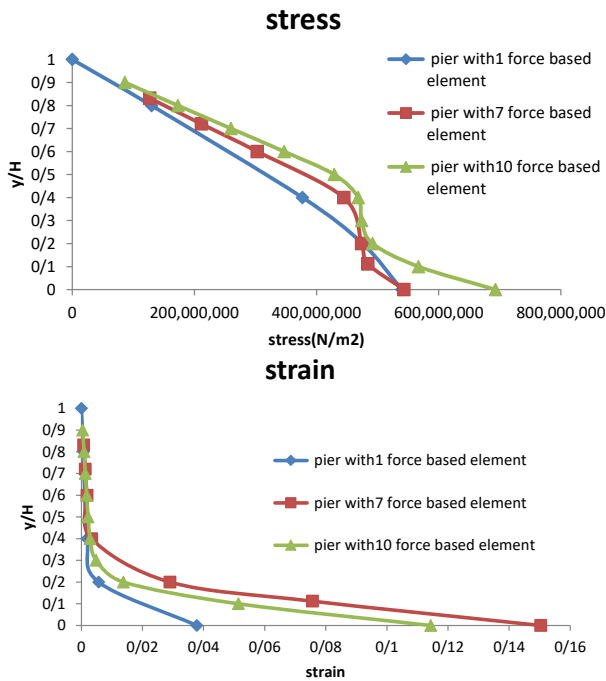


Fig. 23 Comparison between steel strain and stress using 1, 7, 10 force-based elements over the length of the bridge pier at 20.0% of maximum displacement

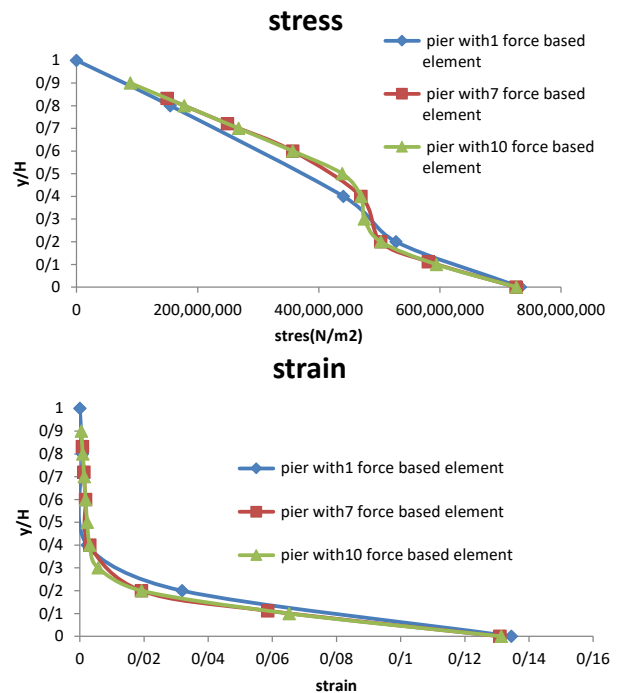


Fig. 25 Comparison between steel strain and stress using 1, 7, 10 force-based elements over the length of the bridge pier at 80.0% of maximum displacement

hysteresis behavior of reinforced concrete pier to predict the response of beam-column element. The number of integration points is one of the principal parameters for prediction of nonlinear response of elements.

6. Influence of concrete behavioral model on the residual drift demand predictions in nonlinear time history analyses

In order for the prediction of permanent displacement demands, three different models are proposed. Nonlinear dynamics analyses are conducted on the models under the near-fault Loma Prieta, 1989 strong ground motion. The ground motion should be modified by a factor of 2/12 since the studied specimen is scaled down prototype of a real bridge pier. The adjusted Loma Prieta, 1989 near-fault

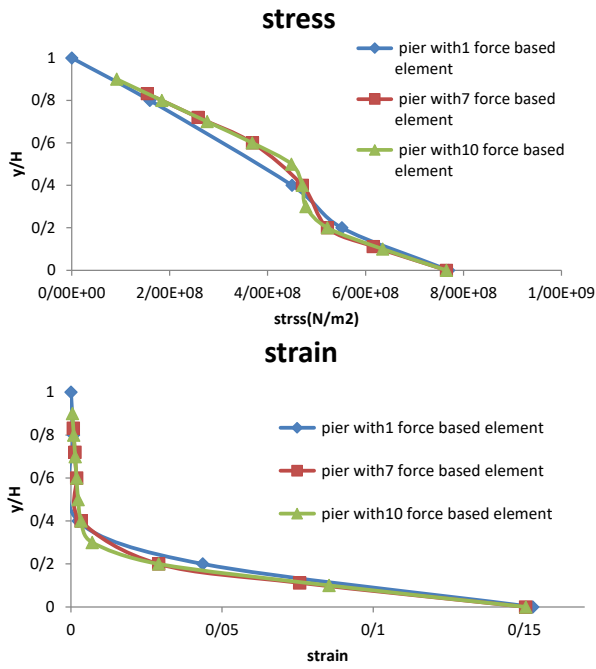


Fig. 26 Comparison between steel strain and stress using 1, 7, 10 force-based elements over the length of the bridge pier at 100.0% of maximum displacement

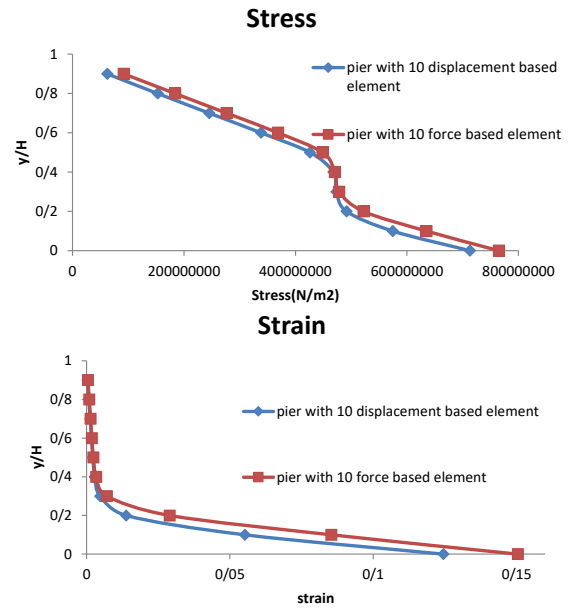


Fig. 28 Comparison of steel stress and strain in the far most tensile fiber over the depth using 10 force-based and displacement elements at 100.0% of the maximum displacement

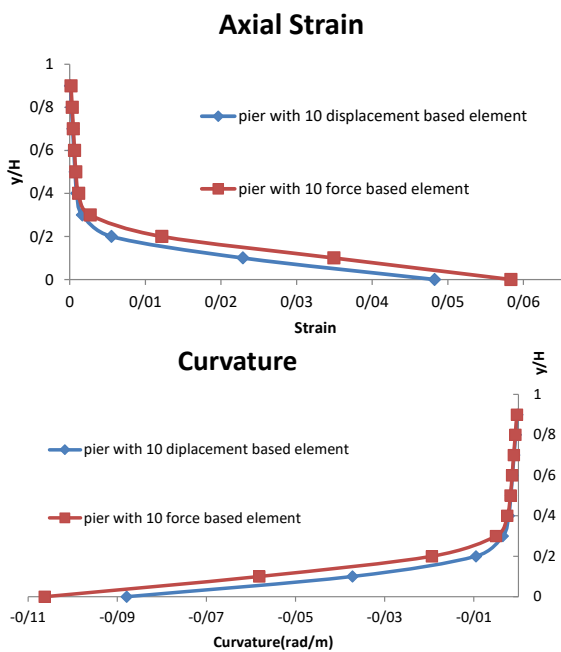


Fig. 27 Axial strain and curvature over the length using 10 force-based and displacement elements at 100.0% of the maximum displacement

ground motion recorded at Los Gatos station is undertaken for the simulation. The result of the simulation is compared with the result of the shake-table test in order for the validation of different models for the prediction of seismic permanent displacement demands. Newmark- β with acceleration constant assumption between time-steps and $\gamma = 0.5, \beta = 0.25$ for nonlinear dynamic analyses is used. The damping ratio is set to be 2% proportional to the

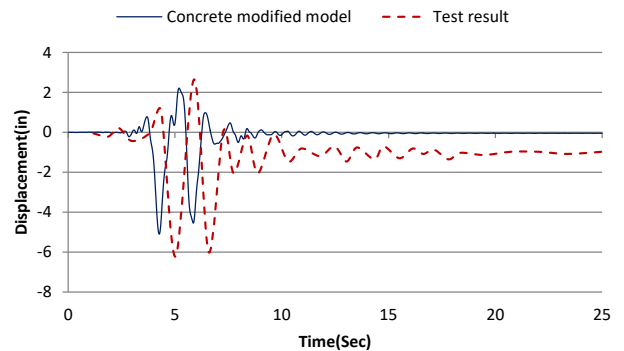


Fig. 29 Comparison of specimen no.1 with shake table test result

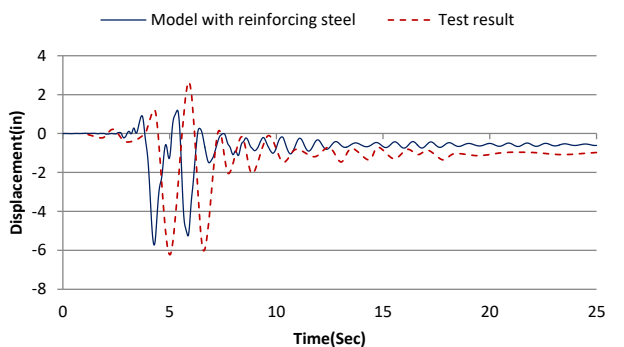


Fig. 30 Comparison of specimen no.2 with shake table test result

stiffness according to the literature (Jeong *et al.* 2008). Simulations presented herein are conducted using the force-based fiber element, which exhibits the highest accuracy according to the study presented in the previous section on the nonlinear static analyses.

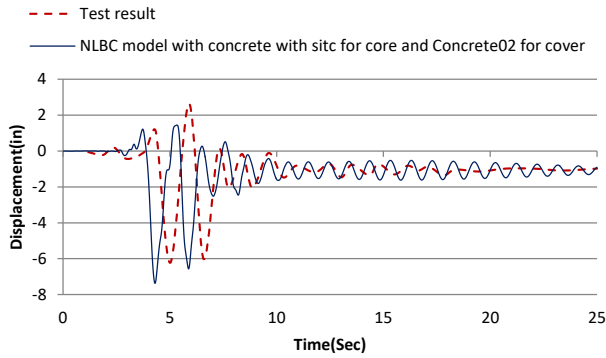


Fig. 31 Comparison of specimen no.3 with shake table test result

Model no. 1 is the distributed plasticity model utilizing 10 elements with 5 integration points in each element. Cover and core concrete are modeled using Concrete01 model. The steel reinforcement is modeled using Giuffre-Menegotto-Pinto (G-M-P) model. The results as shown in Fig. 29 suggest this model does not predict the residual drifts accurately. Even though Gauss Lobatto integration method, which includes integration points at two ends of the element, is used, the unrealistic behavior of the concrete in loading cycles especially within cracked regions of the pier leads to unrealistic prediction of the permanent displacements.

Model no. 2 corresponds to the modeling with distributed plasticity in which 10 elements with 5 integration points in each element is used. Concrete cover and core are modeled using Concrete02 model. This model accounts for the concrete tensile strength and spalling of the concrete cover. The steel reinforcement is modeled using the Reinforcing Steel model which can account for isotropic stiffening and steel strength deterioration parameters. It can take reinforcement buckling between two successive stirrups into account as a function of the reinforcement slenderness through Gomes and Appleton model.

The results as shown in Fig. 30 reveal this model can predict the permanent displacement satisfactorily. The predicted results are smaller than those obtained from shake table test. The predicted maximum displacement is also lower than the that of the test result. It seems the model is stiffer in comparison to the experimental specimen.

Model no.3 is the beam-column distributed plasticity model in which concrete cover is modeled using Concrete02, and the concrete core is modeled using Concrete with SITC. Reinforcing Steel model is used to idealize the transverse reinforcement. The result as shown in Fig. 31 reveals the predicted permanent displacements are in good agreement with the shake table result. The predicted maximum displacement is slightly greater than the shake table experimental maximum displacement. Therefore, it could be concluded the Model no.3 is the best model to predict the permanent displacements of bridge piers. In this study, on the contrary to the previous works in which the reloading strain is chosen as a function of the unloading and the maximum strain, an appropriate interval for the reloading strains is recommended based on the result

of dynamic shake table test and the previous cyclic tests of earlier researches. In this study the reloading strain is selected in range 0.03-0.045.

7. Conclusions

It was found from the result of nonlinear static analyses that displacement-based element required to be refined adequately to be able to predict the curvature and the axial strains with a desirable degree of accuracy. However, the force-based beam-column element displayed a higher level of the accuracy, which can be even improved with incorporating with enough number of integration points.

Simulations using force-based elements with large mesh sizes cannot satisfactorily predict local responses especially within lower levels of lateral deformations.

Incorporation solely with one displacement-based element can result in inaccurate predictions of local responses (e.g., axial strain, curvature, stress, and strain).

It is crucial to incorporate with a discretization scheme including an adequate number of fibers in order to predict local responses satisfactorily. In this regard, the radial meshing of the cross-section typically results in more accurate predictions than unidirectional meshing method.

Both increases in the number of elements and number of integration points in force-based elements lead to increase the accuracy. However, the increase in the number of integration points is usually more preferable from numerical points of view.

Both local and global responses tend to converge more rapidly with the increase of number integration points in force-based elements.

Both Displacement-based and force-based elements can lead to similar results if a proper number of elements and integration points are included.

Even though fiber element modeling can handle prediction of the maximum seismic displacements with a significant degree of accuracy, it cannot handle prediction of permanent displacements satisfactorily which rooted in the stress-strain behavior model of the concrete. The modified concrete model (Concrete with SITC) which is force-based elements employs the unequal unloading and reloading strains, and the path of reloading is modified in a way to start reloading at a strain less than unloading strain (ϵ_r). This process happens due to transfer of the force through tensile cracks because of having them filled with the crushed material in the loading cycles. Selection of the concrete model leads to the augmentation of its capabilities to predict the permanent displacements.

Residual drifts can be predicted with a desirable degree of accuracy if the Stanton-McNiven concrete model and Kent-Scott-Park concrete model is employed for the core concrete and cover concrete, respectively, together with a reinforcing steel model which can account for the reinforcement buckling.

The reloading strain as one of the concrete model parameters plays a prominent role in the accuracy of residual displacement predictions. This parameter can be chosen based on the existing results of cyclic tests or shake table tests of the bridge piers.

References

- Alemdar, B.N. and White, D.W. (2005), "Displacement, flexibility, and mixed beam-column finite element formulations for distributed plasticity analysis", *J. Struct. Eng.*, **131**(12), 1811-1819.
- Alemdar, V.Z., Matamoros, A.B. and Browning, J. (2013), "High-resolution modeling of reinforced concrete bridge columns under seismic loading", *ACI Struct. J.*, **110**(5), 745-754.
- Ansari, M., Ansari, M. and Safiey, A. (2018), "Evaluation of seismic performance of mid-rise reinforced concrete frames subjected to far-field and near-field ground motions", *Earthq. Struct.*, **15**(5), 453-462.
- Ansari, M., Daneshjoo, M. and Soltani, M. (2017), "On Estimation of seismic residual displacements in reinforced concrete single-column bridges through force-displacement method", *Int. J. Civil Eng.*, **15**(4), 473-486.
- Bahadori, A. and Ghassemieh, M. (2016), "Seismic evaluation of I-shaped beam to box-column connection with top and seat plates by the component method", *SHARIF: Civil Eng.*, **322**(21), 129-138.
- Bas, S. and Kalkan, I. (2016), "The effect of vertical earthquake motion on an R/C structure", *Struct. Eng. Mech.*, **59**(4), 719-737.
- Beery, M.P. and Eberhand, M.O. (2008), "Performance modeling strategies for modern reinforced concrete bridge columns", PEER Report 2007/07, Pacific Earthq. Eng. Res. Center, Univ. of California, Berkeley, U.S.A.
- Calabrese, A., Almeida, J.P. and Pinho, R. (2010), "Numerical issues in distributed inelasticity modeling of RC frame elements for seismic analysis", *J. Earthq. Eng.*, **14**(S1), 38-68.
- Choi, H., Saiidi, S., Somerville, P. and El-Azizy, S. (2010), "Experimental study of reinforced concrete bridge columns subjected to near-fault ground motions", *ACI Struct. J.*, **107**(1), 3-12.
- Du, K., Sun, J. and Xu, W. (2012), "The division of element, section and fiber in fiber model", *J. Earthq. Eng. Eng. Vibr.*, **32**(5), 39-46.
- Fahmy, M., Wu, Z., Wu, G. and Sun, Z. (2010), "Post-yield stiffness and residual deformations of RC bridge columns reinforced with ordinary rebars and steel fiber composite bars", *J. Eng. Struct.*, **124**(32), 2969-2983.
- Guyen, P.C. and Kim, S.E. (2014), "Distributed plasticity approach for time-history analysis of steel frames including nonlinear connections", *J. Constr. Steel Res.*, **100**, 36-49.
- Hashemi, S.S. and Vaghefi, M. (2015), "Investigation of bond slip effect on the P-M interaction surface of RC columns under biaxial bending", *Sci. Iran J. Trans. A*, **22**(2), 388-399.
- Huang, X. and Kwon, O. (2015), "Numerical models of RC elements and their impacts on seismic performance assessment", *Earthq. Eng. Struct. Dyn.*, **44**, 283-298.
- Huang, Z.M. and Chen, T. (2003), "Comparison between flexibility-based and stiffness-based nonlinear beam-column elements", *Eng. Mech.*, **20**(5), 24-31.
- Huff, T. (2016), "Estimating residual seismic displacement for bilinear oscillators", *Pract. Periodic. Struct. Des. Constr.*, **21**(2), 04016003-1-11.
- Jeong, H.I., Sakai, J. and Mahin, S.A. (2008), "Shaking table tests and numerical investigation of self-centering reinforced concrete bridge columns", PEER Report 2008/06, Pacific Earthq. Eng. Res. Center, Univ. of California, Berkeley, California, U.S.A.
- Kampitsis, A.E., Giannakos, S., Gerolymos, N. and Sapountzakis, E.J. (2015), "Soil-pile interaction considering structural yielding: Numerical modeling and experimental validation", *Eng. Struct.*, **99**, 319-333.
- Karaton, M. (2014), "Comparisons of Elasto-fiber and fiber & Bernoulli-Euler reinforced concrete beam-column elements", *Struct. Eng. Mech.*, **51**(1), 89-110.
- Karsan, I.D. and Jirsa, J.O. (1969). "Behavior of concrete under compressive loading", *ASCE J. Struct. Div.*, **95**(ST-12).
- Lee, W.K. and Billington, S. (2010), "Modeling residual displacement of concrete bridge columns under earthquake loads using fiber elements", *J. Brid. Eng.*, **15**(3), 240-249.
- Li, S., Zhai, CH. and Xie, L.L. (2012), "Evaluation of displacement-based, force-based and plastic hinge elements for structural non-linear static analysis", *Adv. Struct. Eng.*, **15**(3), 503-514.
- Mander, J.B. and Cheng, C.T. (1997), "Seismic resistance of bridge piers based on damage avoidance design", Report No. NCEER-97-0014, Department of Civil and Environmental Engineering, State University of New York at Buffalo, New York, U.S.A.
- OpenSees (2008), *Open System for Earthquake Engineering Simulation*, <<http://opensees.berkeley.edu>>.
- Petrone, F., Shan, L. and Kunnath, S.K. (2016), "Modeling of RC frame buildings for progressive collapse analysis", *Int. J. Concrete Struct. Mater.*, **10**(1), 1-13.
- Phan, V., Saiidi, S., Anderson, J. and Ghasemi, H. (2007), "Near-fault ground motion effects on reinforced concrete bridge columns", *J. Struct. Eng.*, **133**(7), 982-989.
- Ramin, K. and Fereidoonfar, M. (2015), "Finite element modeling and nonlinear analysis for seismic assessment of off-diagonal steel braced RC frame", *Int. J. Concrete Struct. Mater.*, **9**(1), 89-118.
- Roh, H., Reinhorn, A.M. and Lee, J.S. (2012), "Power spread plasticity model for inelastic analysis of reinforced concrete structures", *Eng. Struct.*, **39**, 148-161.
- Sadeghi, K. and Nouban, F. (2017), "behavior modeling and damage quantification of confined concrete under cyclic loading", *Struct. Eng. Mech.*, **61**(5), 625-635
- Shu, Z. and Zhang, J. (2018), "Dimensional estimation of residual-drift demands for bilinear bridges under near-fault ground motions", *J. Brid. Eng.*, **23**(11), 04018087-1-19.
- Taucer, F.F. and Spacone, E. (1991), "A fiber beam-column element for seismic response analysis of reinforced concrete structures", Report No. UCB/EERC-91-17, Earthquake Engineering Research Center, College of Engineering, University of California, Berkeley, California, U.S.A.
- Terzic, V. (2011), "Force-based element vs. Displacement-based element", Pacific Earthquake Engineering Research Center (PEER), University of California, Berkeley, California, U.S.A.
- Wang, Z., Song, W., Wang, Y. and Wei, H. (2011), "Numerical analytical model for seismic behavior of prestressing concrete bridge column systems", *J. Proc. Eng.*, **14**(7), 2333-2340.
- Zendaoui, A., Kadid, A. and Yahiaoui, D. (2016), "Comparison of different numerical models of RC elements for predicting the seismic performance of structures", *Int. J. Concrete Struct. Mater.*, **10**(4), 461-478.